Food Sci. Biotechnol. 25(1): 97-104 (2016)
DOI 10.1007/s10068-016-0014-x

Food Science
and
Biotechnology

Effects of Reaction Parameters on Self-degradation of L-ascorbic Acid and Self-degradation Kinetics

Ya Li, Yan Yang*, Ai-Nong Yu, and Kui Wang

School of Chemistry & Environmental Engineering, Hubei University for Nationalities, Enshi, 445000, China

Received August 15, 2015
Revised October 27, 2015
Accepted October 27, 2015
Published online February 29, 2016

*Corresponding Author
Tel: +86-718-8437531
Fax: +86-718-8437832
E-mail: yanyang2009@hbmy.edu.cn

pISSN 1226-7708
eISSN 2092-6456

Abstract The degradation behavior of L-ascorbic acid (ASA) was investigated under different parameters of temperature, time, and pH. Higher temperatures and longer times accelerated the ASA degradation. Degradation product distributions changed with different pH values. As solution pH of 4.5 was beneficial for formation of uncolored intermediate products with an absorbance maximum at 294 nm. Formation of brown products was promoted at pH values from 5.8 to 6.8 with an absorbance maximum at 420 nm. Under different pH conditions, volatile products formation varied. Furfural and derivatives of furan were primary products due to the effects of pH. The non-enzymatic self-degradation behavior of ASA was characteristic of first-order kinetics based on a classic dynamic model. Activation energy values varied under different pH values. An ASA degradation mechanism and pathway are proposed.

Keywords: L-ascorbic acid, self-degradation, dynamic

Introduction

L-Ascorbic acid (ASA), also known as vitamin C, is one of the most important human nutritional factors and is used as an additive in many foods due to an anti-oxidant capacity (1,2). Loss of nutrients, such as ASA, can be a critical factor for the shelf life of some products, such as juice, lemons, and vegetables. Degradation of ASA has been considered a major cause of quality and color changes during processing and storage of food products (3,4) and is the source of a brown substance (5,6) that indirectly influences the color and flavor of food. However, ASA is an unstable compound and easily decomposes under less than optimum conditions.

The degradation process of ASA is complex and involves a number of oxidation/reduction and intermolecular rearrangement reactions (3-6). Degradation of ASA proceeds via both aerobic and anaerobic pathways (7,8) depending upon presence of oxygen, heat, and light (9), and storage temperature and time (10,11). However, degradation of ASA mainly results in formation of volatile products (VPs) and brown-products (BPs) via self-degradation and non-enzymatic browning (NEB).

Research focused on self-degradation of ASA is mainly focused on the effects of fruit nutrient compositions (12-14). Degradation kinetics of ASA in citrus juice, lemon juice, guava, and olives have been reported (1,9,15,16). ASA degradation behavior and the effects of temperature and time on the concentration loss of ASA during fruit storage have been investigated (12-16). Degradation of pure ASA has also been investigated (17,18). An explanation for the degradation behavior of ASA remains unknown. The relationship between products and reaction parameters of pH, time, and temperature on the process of ASA degradation has few been reported.

The self-degradation behavior of ASA was investigated in this study. Formation of uncolored intermediate products (UIPs), BPs, and VPs and correlations with the kinetics of ASA degradation are discussed and a possible degradation mechanism and pathway of ASA is proposed.

Material and Methods

Reagents The analytical grade reagents ASA, Na_2HPO_4, NaH_2PO_4, NaOH and the guaranteed reagents meta-phosphate and methanol were purchased from Sinopharm Chemical Reagent Co., Ltd. (Shanghai, China). Standards for use as gas chromatography (GC) reference compounds were obtained from J&K China Chemical Ltd. (Shanghai, China). C_5-C_{22} n-alkanes were obtained from Pure Chemical Analysis Co., Ltd (Bornew, Belgium). Water was re-distilled before use.

Experimental procedure A model reaction system and pH values were used based on previous reports (19-21). ASA (0.50 mmol) was dissolved in 10 mL of different buffer solutions adjusted to 4.5, 5.8, 6.8, 8.0, 9.5 pH using the solvents 0.20 M Na_2HPO_4, 0.20 M NaH_2PO_4, and 0.20 M Na_2HPO_4-NaH_2PO_4 with a pH meter (PB-21; Sartorius AG

Inc., Beijing, China). Reactants were sealed in 15 mL Synthware® pressure glass vials (Beijing Synthware Glass, Inc., Beijing, China) and heated with stirring (DF-101S; Shanghai Qiang Qiang Equipment Co., Ltd., Shanghai, China) at different temperatures and times in a heated oil bath (4,20). Temperatures and times ranged from 110 to 150°C and from 10 to 150 min, respectively. The reactor was removed from the heated oil bath and immersed in an ice water bath to stop the reaction when the desired reaction time had elapsed. Experimental errors were estimated at least in triplicate under identical conditions, and each data point was reported as a mean value of 3 experimental results.

Measurement Methods

***Determination of the ASA concentration*:** The ASA concentration in solution was determined based on reverse phase (RP) HPLC using a model 1260 apparatus (Agilent, Santa Clara, CA, USA), equipped with a UV diode array detector and a C_{18} column (3.5 μm, 4.6 mm i.d.×100 mm). Detection conditions were mobile phase elution composed of 0.1 weight percent (wt. %) water/methanol/meta-phosphate using gradient elution mode (21). The flow rate was 1.0 mL/min, the column temperature was 30°C, the injection volume was 10 μL, and the detection wavelength was 243 nm.

ASA was quantified based on an external standard procedure (21) using a calibration curve of ASA standard sample (correlation coefficient, R^2=0.9998). Each data point was reported as a mean value of 3 experimental determinations. Experiments are carried out at least in triplicate with a relative standard deviation (RSD) less than 4.5%.

***Measurement of UIPs and BPs*:** The UV absorbance and browning of model reaction solutions were measured following a previous method (21). UV absorbance and browning intensity of model reaction solutions were measured at ambient temperature at 294 (22,23) and 420 nm (24) respectively, using a Cary300 spectrophotometer (Shimadzu Co., Ltd., Kyoto, Japan). In order to obtain the highest optical density value, dilutions of 30x-100x/0x-25x were prepared. Experiments were carried out in triplicate. Average RSD values were 4.7 and 4.3% at 294, 420 nm respectively. Final absorbance values at 294 and 420 nm were actual absorbance values multiplied by dilution factors of 30x-100x/0x-25x.

Identification and quantification of VPs using headspace-solid-phase micro-extraction (SPME)-GC-MS Quantitative and qualitative analyses were performed using a 6890N GC apparatus (Agilent) and an Agilent 6890N-5975i GC-MS apparatus, respectively. VPs were analyzed using headspace-SPME-GC-MS spectrometry following previously reported conditions (5) for degradation of ASA. VPs were extracted using headspace-SPME equipped with Carboxen/Poly-dimethylsiloxane (CAR/PDMS) (75/30 μm thickness) (Supelco, Bellefonte, PA, USA) (25). The extraction time was 30 min at 50°C.

An Agilent 6890N gas chromatograph coupled with an Agilent 5975i mass selective detector was used for VPs identification. VPs were separated using an HP-5 capillary column (30 m×0.25 mm i.d.×0.25 mm). Before analysis, an SPME fiber was desorbed and maintained in the injection port at the oven temperature of 250°C for 4.0 min, as suggested by the manufacturer. The temperature program was isothermal for 5 min at 40°C, raised to 260°C at a rate of 5°C/min, then raised to 280°C at a rate of 15°C/min, and holding for 1 min (20-22). Linear retention indices (LRI) were calculated based on detection of C_5-C_{22} n-alkanes under the same chromatographic conditions and were used to identify detected compounds. The transfer line to the mass spectrometer was maintained at 280°C. Mass spectra were obtained using a mass selective detector with a 70 eV electronic impact, a 1,753 V multiplier voltage, and a 1 scan/s data collection rate over an m/z range of 30-400 amu. VPs were identified based on comparison of mass spectra with spectra in the NIST Chemistry Web Book and Wiley 275 libraries (19,20). Similarly, authentic samples were, as far as possible, obtained from the above-mentioned drug companies for determination of the exact class of VPs based on comparison of LRI values.

Kinetic modeling Previous reports of traditional kinetics theory used in food chemistry studies exist (26-28). In a closed system with only 1 compound reacting, disappearance of a compound would follow Eq. (1):

$$-\frac{d[A]}{dt} = k[A]^n \qquad \text{Eq. (1)}$$

The decreasing concentration of *A* over time *t* is related closely to the concentration of the reacting component, where *k* is the reaction rate constant and *n* is the reaction order, which usually ranges from 0 to 2. Considering the effects of variant parameters and integration of different equations to the proper order with respect to time, the zero-order reaction would be:

$$[A]-[A]_0 = -kt \qquad \text{Eq. (2)}$$

The first-order reaction would be:

$$\frac{[A]}{[A]_0} = \exp(-kt) \qquad \text{Eq. (3)}$$

The second-order reaction would be:

$$\frac{1}{[A]}-\frac{1}{[A_0]} = -kt \qquad \text{Eq. (4)}$$

Statistical analysis Data were obtained based on experiments carried out at least in triplicate with RSD within 5.0% in order to control the correlation coefficient (R^2)>0.99. All data were processed using Microsoft Office 2010 and Orgin 7.5.

Results and Discussion

Initial pH change for degradation of ASA The initial pH change for

ASA degradation at 140°C for different time, which time ranges from 20 to 150 min, is shown in Fig. 1. It's implied that the pH value changed during a long reaction time. When the initial pH>7.0, such as at 8.0 or 9.5, the pH would drop to near to 7.3 with an increasing time. When initial pH<7.0, especially at 6.8, a change of pH was small. As pH is 4.5, when the time ranged from 0 to 40 min, the pH value increased. Although the solution pH had been adjusted using a buffer solution, the pH of the reaction solution was affected by degradation products generated from ASA once the reaction began.

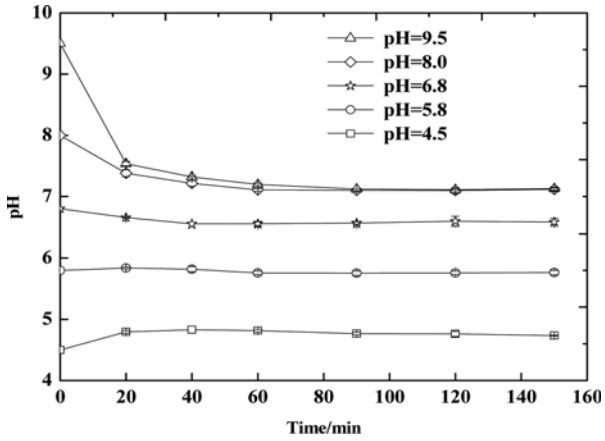

Fig. 1. pH change for ASA degradation at different time in a buffer solution at 140°C.

Effects of temperature, time, and pH on degradation of ASA Effects of temperature, time, and pH on ASA degradation were analyzed. Reaction temperatures were 110, 120, 130, 140, and 150°C and reaction times ranged from 0 to 150 min at initial pH values of 4.5, 5.8, 6.8, 8.0 and 9.5 adjusted using buffer solutions and measured at ambient temperature.

The concentration of ASA decreased with an increasing reaction time under different temperatures and pH values (Fig. 2). When the initial pH value was 4.5, the decrease in the ASA concentration was larger than for other pH values (Fig. 2B, 2C, 2D, and 2E) except for a pH value of 6.8 (Fig. 2A). When the temperature was low at 110°C (Fig. 2A), the decreasing concentration of ASA was smaller than other temperature, especially when the initial pH was 8.0 or 9.5. As time reached 150 min, concentrations of ASA were 7.410 and 7.584 mg/mL for initial pH values of 8.0 and 9.5, which were less than the values of the primary ASA concentration of approximately 8.820 mg/mL. When the temperature changed from 120 to 150°C, the effect of pH=4.5 was strongest with a lesser effect at pH=5.8 and a weak effect at pH=9.5. The decreasing rate of the ASA concentration increased as the reaction time increased and the temperature increased at different pH values. When the pH value was 4.5, the concentration of ASA ranged from 7.755 to 1.275 mg/mL. When the pH value was 9.5, the concentration of ASA changed from 8.808 to 6.245 mg/mL at 120°C (Fig. 2B). However, primary regions of changes were from 5.635 to 0.030 mg/mL and 7.695 to 0.474 mg/mL at pH values of 4.5 and 9.5 at 150°C, respectively, (Fig. 2E). When the reaction time was long enough, the curve of the decreasing ASA concentration became smoothly.

Both a change in temperature and a change in the primary pH value of the solution can account for these results. With an increasing temperature, the environment of the solution changed (29) and as temperature increased, the pKa value declined to less than the value under ambient temperature. Therefore, at 150°C, the concentration of ASA decreased faster than under other temperatures for the same time period.

For the primary pH value, the environment of the solution changed as the reaction proceeded (26). Although the primary pH value of the solution was adjusted using a buffer solution, the pH value of solution changed due to degradation of ASA (Fig. 1). Martins and Boekel (26) reported that the pH value would change when the primary solution pH>7.0. In this study, when the primary pH=9.5, as time elapsed the pH value of the solution was <8.0 at 140°C, while the pH value of the solution was not seriously influenced when the primary pH ranged from 4.5 to 5.8 (Fig. 1).

In an acidic environment the stability of ASA changes, which would be the situation with fluctuation of the pH value. Xie (30) reported that the concentration of ASA decreased fastest at pH=4.0, and when the solution pH ranged from 2.2 to 6.0, ASA would mostly be degraded to dioxide and furaldehyde. Thus, degradation of ASA was strongly influenced by the solution pH and the reaction temperature. High temperatures and low pH values promoted degradation of ASA.

Correlations between absorbance values of UIPs and BPs, and the ASA concentration Correlations between absorbance values of UIPs and BPs and the concentration of ASA at 110 and 150°C and pH values of 4.5, 5.8, 6.8, 8.0 and 9.5 are shown in Fig. 3. The concentration of ASA decreased and the absorbance of UIPs and BPs increased at both temperatures and different pH values. It's suggested higher temperature and lower pH intensified degradation of ASA (Fig. 2). When the pH was 4.5 (Fig. 3A) with a reaction time of 10-150 min, the absorbance value at 294 nm ($A_{294\ nm}$) increased from 2.80 to 13.92 at 110°C. While within the same reaction time, $A_{294\ nm}$ values ranged from 11.63 to 45.49 at 150°C. When the pH was 9.5, the $A_{294\ nm}$ value ranged from 2.12 to 6.34 at 110°C, while the value ranged from 4.71 to 24.13 at 150°C (Fig. 3E). At both 110 and 150°C for pH values was of 5.8, 6.8 and 8.0, the $A_{294\ nm}$ value was less than that value at pH=4.5. Thus, an increasing temperature and a decreasing solution pH value promoted formation of UIPs. The $A_{420\ nm}$ value still increased as time and temperature increased under different experimental pH values. However, the impact of pH on the $A_{420\ nm}$ value was contrary to $A_{294\ nm}$ values. At 110°C, the $A_{420\ nm}$ value was higher at 6.8 than at other pH values. Nevertheless, at 150°C and pH=5.8, the $A_{420\ nm}$ value was much higher than at other pH values with time>40 min. When reaction time>120 min, $A_{294\ nm}$ and $A_{420\ nm}$ values did not change.

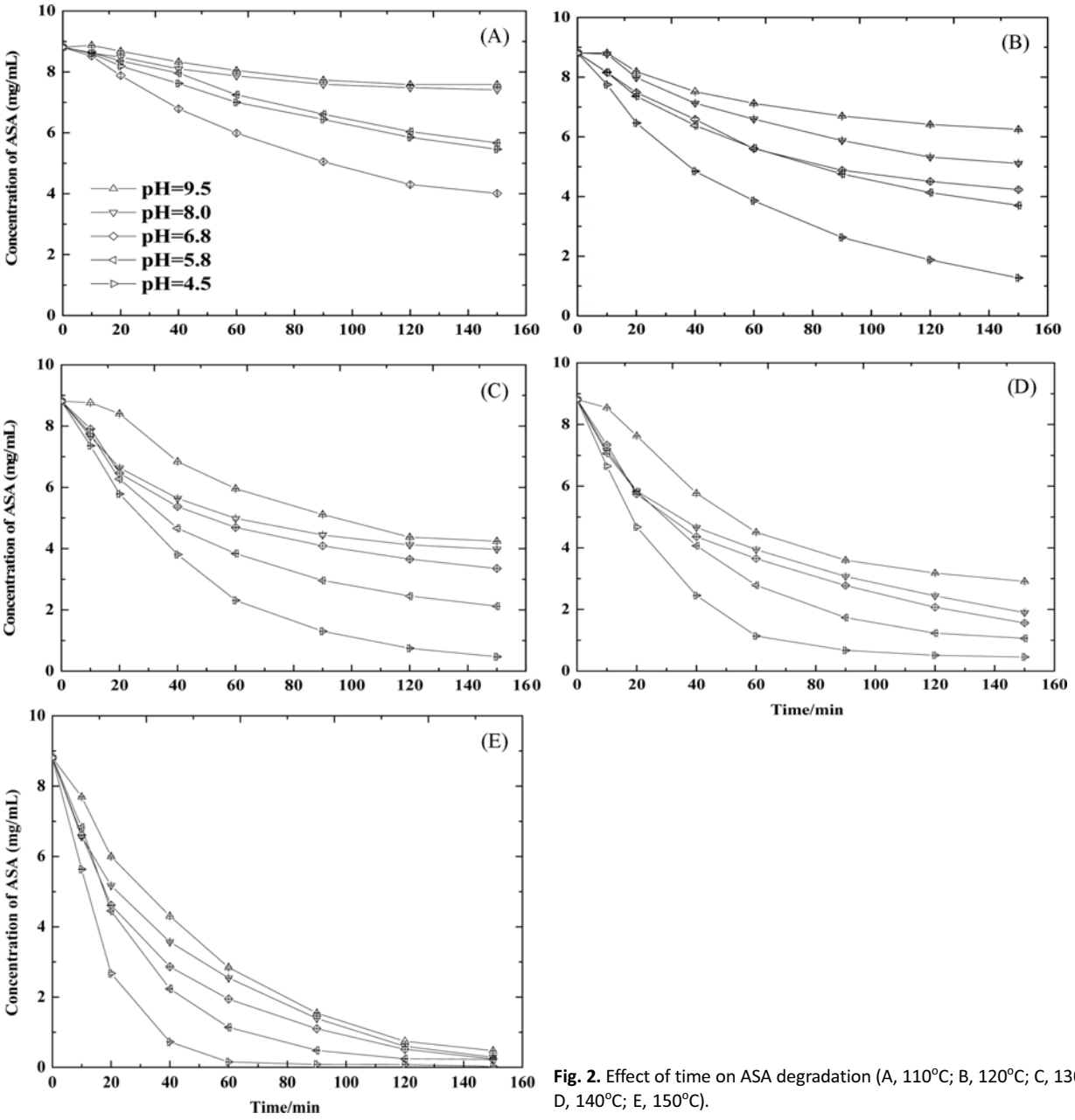

Fig. 2. Effect of time on ASA degradation (A, 110°C; B, 120°C; C, 130°C; D, 140°C; E, 150°C).

Based on mutative tendencies of $A_{294\ nm}$ and $A_{420\ nm}$ values and decreasing ASA concentrations under experimental parameters (time, temperature, and pH) (Fig. 3), absorbance values of UIPs were higher than values of BPs, which also indicates that the $A_{294\ nm}$ value was much higher than the $A_{420\ nm}$ value as ASA was consumed. Based on an ASA degradation mechanism (4,31,32) and results reported herein, ASA first degrades to UIPs, which are generally used to determine intermediate compounds in the non-enzymatic browning reaction (33). When the concentration of UIPs is high enough, BPs can be generated so that UIPs would be regarded as precursors of BPs (34). The solution color became a much darker brown when the reaction lasted for a long time in this study.

VPs from degradation of ASA VPs formed during degradation of ASA were studied using headspace-SPME-GC-MS spectrometry with experimental parameters for ASA degradation of 150°C and 120 min under pH values of 4.5, 5.8, 6.8, 8.0 and 9.5. The total ion peak area of volatility is shown in Table 1.

VPs formed during ASA degradation were influenced by the initial pH, revealing that the mechanism of ASA degradation was dependant on reaction parameters. Under acidic conditions, especially at pH=4.5, VPs from ASA degradation were mainly furfural. However, with an increasing pH, less and less furfural was generated. When pH ranged from 6.8 to 9.5, there was no furfural identified. The VPs 2-methyl-furan and 2-acetyl-5-methyl-furan were generated under

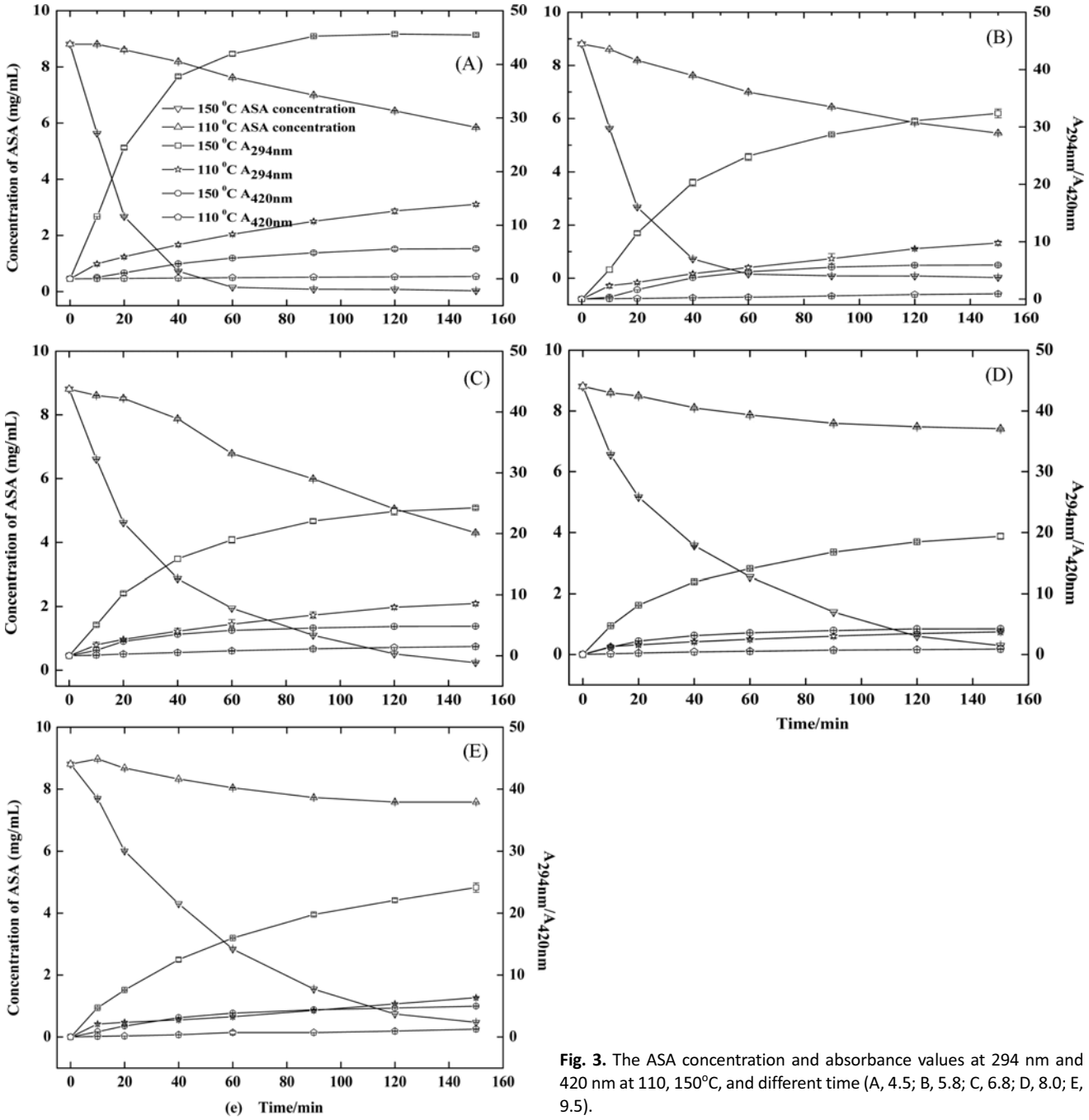

Fig. 3. The ASA concentration and absorbance values at 294 nm and 420 nm at 110, 150°C, and different time (A, 4.5; B, 5.8; C, 6.8; D, 8.0; E, 9.5).

alkaline conditions. However, some VPs would easily auto-react or react with other products under alkaline conditions in solution. VPs varieties were reduced in diversity and yields were higher under an acid environment, contrary to an alkaline environment (Table 1).

Degradation kinetics of ASA Degradation kinetics of ASA were investigated when temperature ranged from 110 to 150°C with pH values of 4.5, 5.8, 6.8, 8.0 and 9.5. Rate constants (k) as a function of heating time for a decreasing ASA concentration are summarized in Table 2.

ASA degradation occurs via 2 main mechanisms. Under diverse temperatures and pH values, ASA is converted to VPs and UIPs in different ways. Retention concentration of ASA can be used in a kinetic model based on Eq. 2, 3, and 4 for calculation of rate constants (k). Based on the value of k and the correlation coefficient (R^2), degradation of ASA follows first-order reaction kinetics, in agreement with results reported by Montano *et al*. (16) and Bree *et al*. (35).

The rate constant k increases with an increasing reaction temperature under different pH values. The 2 factors for ASA degradation were reaction temperature and solution pH. With an initial solution pH value of 4.5, 5.8, 6.8, 8.0 and 9.5 using a buffer, the

Table 1. Influence of pH on formation of VPs from ASA degradation (GC-MS peak areas×10^6)

	Compounds		LRI	Identification	pH 4.5	pH 5.8	pH 6.8	pH 8.0	pH 9.5
	Substances	Construction							
1	2,2,-methylenebis-furan	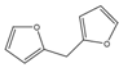	1086	MS,LRI	50.25	ND	ND	ND	ND
2	2,2′-bifuran	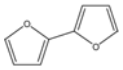	1038	MS,LRI	5.07	ND	ND	ND	ND
3	furfural	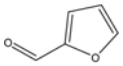	835	MS,LRI, Co-GC	301.39	30.75	ND	ND	ND
4	3-ethyl-2-hydroxy-2-cyclopenten-1-one	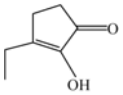	1082	MS,LRI	3.99	10.65	15.76	ND	ND
5	2-methyl-furan	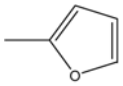	604	MS,LRI	ND	15.27	29.52	19.75	25.54
6	2,4- dimethyl-furan	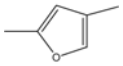	713	MS,LRI	ND	4.99	10.99	1.98	1.17
7	2-methyl-2-cyclopenten-1-one	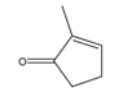	912	MS,LRI	ND	ND	2.52	1.93	3.66
8	2-acetyl-5-methyl-furan	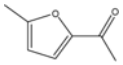	978	MS,LRI, Co-GC	ND	ND	2.76	3.01	7.65
9	carbon dioxide		<500	MS,LRI	7.16	7.12	6.71	5.35	6.05
10	acetone		<500	MS,LRI,	ND	ND	ND	16.54	20.07
	Total peak areas				367.86	68.78	68.26	48.56	64.14

system environment would change for initiation of the reaction. In water, the solution pH is changed when the temperature increases (29). Thus, the effect of temperature was dominant for ASA degradation in the reaction system (Table 2). Therefore, ASA degradation followed the classic Arrhenius formula (26-28).

Based on a first order model of ASA degradation, the fitting lnk vs. 1/T under different pH values was studied. The activation energy (Ea) of ASA degradation was estimated on the basis of an Arrhenius relationship described in Eq. (5).

$$k = A\exp(-E_a/RT) \quad \text{Eq. (5)}$$

Based on fitting lnk vs. 1/T, an initial solution pH of 6.8 was best for promotion of ASA degradation with the activation energy (Ea) of 46.88 kJ/mol. The influence of other pH values was inferior for ASA degradation. When the pH was 4.5 or 9.5, Ea values was 77.79 and 93.33 kJ/mol, respectively. Based on kinetic modeling, the appropriate pH was 6.8 for self-degradation of ASA.

Degradation mechanism of ASA A possible ASA degradation mechanism and pathway are shown in Fig. 4. The degradation mechanism of ASA was investigated based on qualitative analysis of VPs (Table 2). The presence of an adjacent second enol structure causes ASA to easily oxidize and decompose. Firstly, ASA oxidizes into dehydro-ascorbic acid (DHASA), then DHASA hydrolyzes and the ring cleaves into 2, 3-diketone-1-guloacid, which decomposes into aldopentose, and converts into 1-deoxypentosone via isomerization, and 1-deoxypentosone decomposes into minor products. Final products would vary under different initial solution pH values. Under alkaline conditions, 2-methyl-furan, 2, 4-dimethyl-furan, 2-acetyl-5-methyl-furan, and 2-methyl-2-cyclopenten-1-one are the main products, which are UIPs. Under acidic conditions, furfural and derivatives of furan are the main products. Derivatives of furan are 2, 2-methylenbis-furan, 2-methyl-furan, and 2, 4-dimethyl-furan, which are UIPs that eventually polymerize into BPs to cause the solution to become dark and directly affect the nutritional quality of food. The proposed ASA degradation mechanism and pathway showed that the process of ASA degradation is complicated. Further study is required for a better understanding.

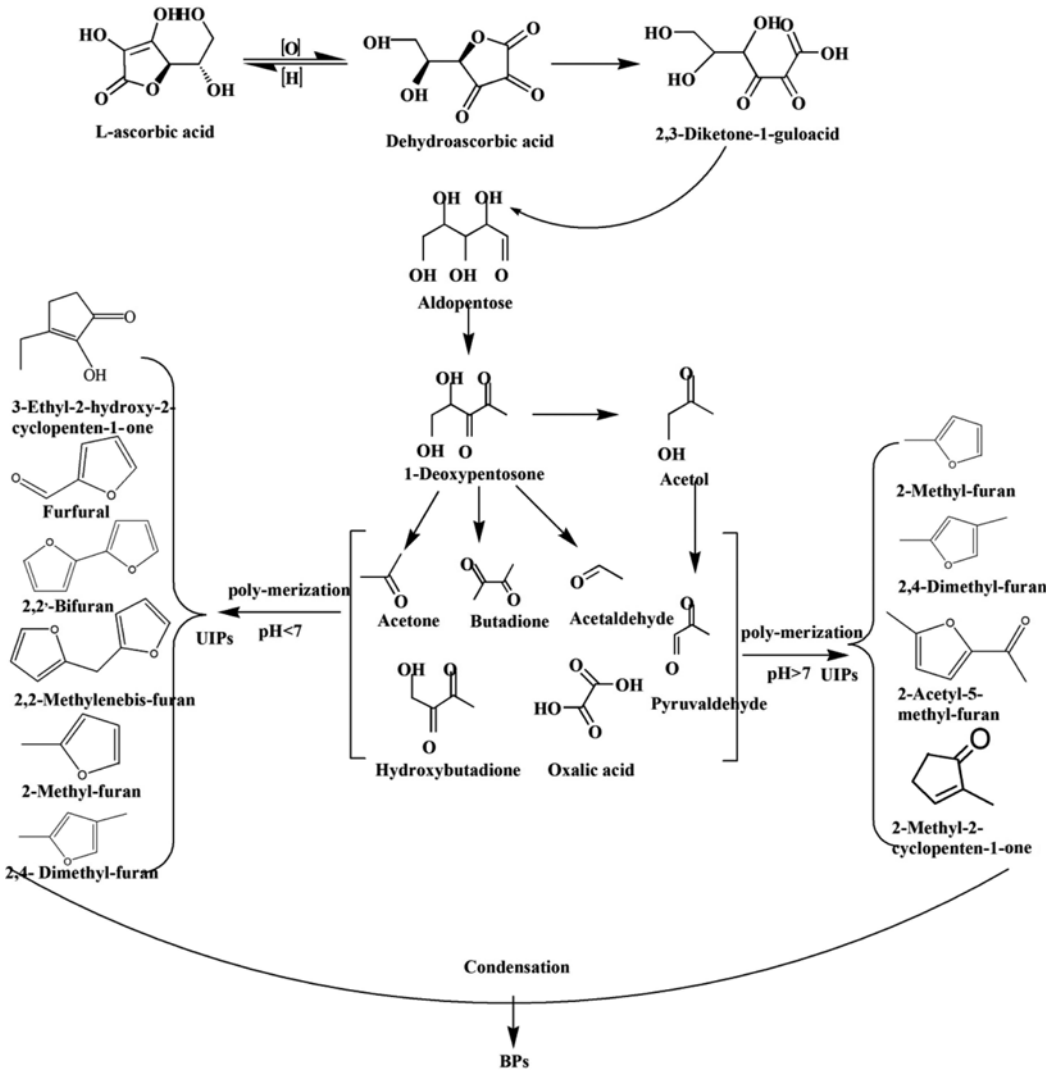

Fig. 4. A possible ASA degradation mechanism and pathway.

Acknowledgments Project 31360408 supported by the National Natural Science Foundation of China, project 2014CFC1126 supported by the Natural Science Foundation of Hubei Province, China, project 14HBZ012 supported by National Committee of China, project PY201502 supported by a Master's Degree Thesis of Hubei University for Nationalities, and the Project of Dominant and Characteristic Discipline Group for Hubei Provincial Universities (Hubei degree 2015-5) all supported this research.

Disclosure The authors declare no conflict of interest.

References

1. Burdurlu HS, Koca N, Karadeniz F. Degradation of vitamin C in citrus juice concentrates during storage. J. Food Eng. 74: 211-216 (2006)
2. Marfil PHM, Santos EM, Telis VRN. Ascorbic acid degradation kinetics in tomatoes at different drying conditions. LWT-Food Sci. Technol. 41: 1642-1647 (2008)
3. Yuan JP, Chen F. Degradation of ascorbic acid in aqueous solution. J. Agr. Food Chem. 46: 5078-5082 (1998)
4. Yu AN, Tan ZW, Wang FS. Mechanism of formation of sulphur aroma compounds from L-ascorbic acid and L-cysteine during the Maillard reaction. Food Chem. 132: 1316-1323 (2012)
5. Yu AN, Tan ZW, Wang FS. Mechanistic studies on the formation of pyrazines by Maillard reaction between L-ascorbic acid and L-glutamic acid. LWT-Food Sci. Technol. 50: 64-71 (2013)
6. Sonali SB, Sandip BB. Non-enzymatic browning in citrus juice: Chemical markers, their detection and ways to improve product quality. J. Food Sci. Tech.-Mys. 51: 2271-2288 (2014)
7. Huelin FE. Studies on the anaerobic decomposition of ascorbic acid. J. Food Sci. 18: 633-639 (1953)
8. Nius D, Wiqle M, Kelly PM, Kipp BH, Schlegel B. Mechanism of ascorbic acid oxidation by cytochrome b_{561}. Biochemistry-US 40: 11905-119011 (2001)
9. Robertson GL, Samaniego CML. Effect of initial dissolved oxygen levels on the degradation of ascorbic acid and the browning of lemon juice during storage. J. Food Sci. 51: 184-187 (1986)
10. Fellers PJ, Carter RD, Dejager G. Influence of the ratio of degrees brix to percent acid on consumer acceptance of processed modified grapefruit juice. J. Food Sci. 53: 513-515 (1988)
11. Gordonl R, Christine SE. Effect of soluble solids and temperature on ascorbic acid degradation in lemon juice stored in glass bottles. J. Food Quality 13: 361-374 (1990)
12. Sapei L, Hwa L. Study on the kinetics of vitamin C degradation in fresh strawberry juice. Procedia Chem. 9: 62-68 (2014)
13. Gabriel AA, Cayabyab JEC, Tan AKL, Corook MLF, Ables EJO, Tiangson-Bayaga CLP. Development and validation of a predictive model for the influences of selected product and process variables on ascorbic acid degradation in

Table 2. Kinetic degradation data of ASA dependence of 2 kind dynamic models under different temperature and pH values

pH	temperature (°C)	Zero-order k (*R*)[1)]	First-order k (*R*)	Second-order k (*R*)
4.5	110	0.0230 (0.9894)	0.0035 (0.9989)	0.0004 (0.9992)
	120	0.0490 (0.9576)	0.0078 (0.9998)	0.0034 (0.9870)
	130	0.0540 (0.9237)	0.0110 (0.9990)	0.0127 (0.9557)
	140	0.0506 (0.8565)	0.0214 (0.9921)	0.0181 (0.9881)
	150	0.0457 (0.7548)	0.0379 (0.9511)	0.1215 (0.9651)
5.8	110	0.0221 (0.9934)	0.0031 (0.9969)	0.0004 (0.9761)
	120	0.03363 (0.9697)	0.0058 (0.9912)	0.0004 (0.9771)
	130	0.0427 (0.9252)	0.0092 (0.9979)	0.0024 (0.9731)
	140	0.0490 (0.9212)	0.0160 (0.9959)	0.0059 (0.9922)
	150	0.0519 (0.8555)	0.0307 (0.9997)	0.0292 (0.9703)
6.8	110	0.0380 (0.9861)	0.0032 (0.9975)	0.0010 (0.9791)
	120	0.0306 (0.9549)	0.0048 (0.9912)	0.0009 (0.9743)
	130	0.0339 (0.9161)	0.0067 (0.9951)	0.0011 (0.9838)
	140	0.0440 (0.9284)	0.0097 (0.9984)	0.0030 (0.9862)
	150	0.0570 (0.8908)	0.0128 (0.9983)	0.0087 (0.9825)
8.0	110	0.0096 (0.9566)	0.0017 (0.9920)	0.0002 (0.9940)
	120	0.0208 (0.8577)	0.0032 (0.9814)	0.0004 (0.9424)
	130	0.0240 (0.9165)	0.0067 (0.9951)	0.0009 (0.9689)
	140	0.0345 (0.9551)	0.0105 (0.9695)	0.0025 (0.9887)
	150	0.0517 (0.9649)	0.0220 (0.9974)	0.0064 (0.9736)
9.5	110	0.0110 (0.9233)	0.0015 (0.9916)	0.0001 (0.9564)
	120	0.0171 (0.9420)	0.0023 (0.9965)	0.0003 (0.9690)
	130	0.0336 (0.9557)	0.0055 (0.9967)	0.0009 (0.9892)
	140	0.0396 (0.9280)	0.0129 (0.9960)	0.0017 (0.9897)
	150	0.0496 (0.9426)	0.0203 (0.9987)	0.0136 (0.9480)

[1)]*R* is the correlation coefficient.

simulated fruit juice. Food Chem. 177: 295-303 (2015)
14. Tiwari BK, Donnell CPO, Muthukumarappan K, Cullen PJ. Ascorbic acid degradation kinetics of sonicated orange juice during storage and comparison with thermally pasteurized juice. LWT-Food Sci. Technol. 42: 700-704 (2009)
15. Uddin MS, Hawlader MNA, Luo D, Mujumdar AS. Degradation of ascorbic acid in dried guava during storage. J. Food Eng. 51: 21-26 (2002)
16. Montano A, Casado FJ, Rejano L, Sanchez AH, de Castro A. Degradation kinetics of the antioxidant additive ascorbic acid in packed table olives during storage at different temperatures. J. Agr. Food Chem. 54: 2206-2210 (2006)
17. Hsu HY, Tsai YC, Fu CC, Wu JSB. Degradation of ascorbic acid in ethanolic solutions. J. Agr. Food Chem. 60: 10696-10701 (2012)
18. Grudiæ VV, Blagojeviæ NZ, Bra̧anac SR. Kinetics of degradation of ascorbic acid by cyclic voltammetry method. Chem. Ind. Chem. Eng. Q. 21: 351-357 (2015)
19. Yu AN, Zhang AD. The effect of pH on the formation of aroma compounds produced by heating a model system containing L-ascorbic acid with L-threonine/L-serine. Food Chem. 119: 214-219 (2010)
20. Yu AN, Tan ZW, Shi BA. Influence of the pH on the formation of pyrazine compounds by the Maillard reaction of L-ascorbic acid with acidic, basic and neutral amino acids. Asia-Pac. J. Chem. Eng. 7: 445-462 (2012)
21. Tang LP, Zhou YY, Yu AN, Comparison of UV spectrophotometry and HPLC in determination of ascorbic acid in Maillard reaction. Sci. Tech. Food Ind. (China) 10: 79-82 (2014)
22. Zhou YY, L Y, Yu AN. Optimum extraction conditions for pyrazine compounds from Maillard reaction mixture by headspace solid-phase microextraction. Food Sci. (China) 36: 119-123 (2015)
23. Yu X, Zhao M, Hu J, Zeng ST, Bai XL. Correspondence analysis of antioxidant activity and UV–Vis absorbance of Maillard reaction products as related to reactants. LWT-Food Sci. Technol. 46: 1-9 (2012)
24. Barbanti D, Mastrocola D, Lerici CR. Early indicators of chemical changes in foods due to enzymic or non enzymic browning reactions. III. Colour change in heat-treated model systems [J]. Food Sci. Tech. 23: 494-498 (1990)
25. Billaud C, Brun S, Louarme L. Effect of glutathione and Maillard reaction products prepared from glucose or fructose with glutathione on polyphenoloxidase from apple-I: Enzymatic browning and enzyme activity inhibition. Food Chem. 84: 223-233 (2004)
26. Martins SIFS, Boekel MAJSV. Kinetics of the glucose/glycine Maillard reaction pathways: Influences of pH and reactant initial concentrations. Food Chem. 92: 437-448 (2005)
27. Martins SIFS, Boekel MAJSV. A kinetic model for the glucose/glycine Maillard reaction pathways. Food Chem. 90: 257-269 (2005)
28. Baisier WM, Labuza TP. Maillard browning kinetics in a liquid model system. J. Agr. Food Chem. 40: 707-713 (1992)
29. Marshall WL, Frank EU. Ion product of water substances, 0-1000, 1-10,000 bars, new international formulation and its background. J. Phys. Chem. Ref. Data 10: 295-304 (1981)
30. Xie MY. Food Chemistry. Chemical Industry Press, Beijing, China. pp. 200-215 (2011)
31. Mareen SMAG. Maillard degradation pathways of vitamin C. Angew. Chem. Int. Ed. 125: 1-6 (2013)
32. Rizzi GP. Role of phosphate and carboxylate ions in mallard browning. J. Agr. Food Chem. 52: 953-957 (2004)
33. Benjakul S, Lertittikul W, Bauer F. Antioxidant activity of Maillard reaction products from a porcine plasma protein–sugar model system. Food Chem. 93: 189-196 (2005)
34. Wu S, Qin J. Study on the mechanism of Maillard reaction. J. Guizhou Univ. Technol. (Natural Science) 34: 17-20 (2005)
35. Bree IV, Baetens JM, Samapundo S, Devlieghere F, Laleman R. Modelling the degradation kinetics of vitamin C in fruit juice in relation to the initial headspace oxygen concentration. Food Chem. 134: 207-214 (2012)